Received: 7/11/2024/Accepted: 22/02/2025

Determination of the microstructural hardening effect on deformed chips in the turning process

Determinación del efecto del endurecimiento microestructural en las virutas deformadas en el proceso de torneado

Andier Samiñón Durán asaminond@ismm.edu.cu [(1)]
Roxana Pupo Matos rpmatos@ismm.edu.cu [(1)]
Odalvis Samiñón Durán osduran@gmail.com [(1)]
Liliana Samiñón Fuentes saminonliliana@gmail.com [(1)]
Iker Cesar Trutié Cobas trutiecobas@gmail.com [(1)]
[(1)] University of Moa, Moa, Cuba

Abstract: The effect of the microstructural hardening phenomenon on deformed chips under different cutting regimes was determined in an AISI 4340 steel subjected to the turning process. A steel rod was subjected to the chip removal process with number of revolutions of 125, 150, 175 and 200 rpm; cutting depths of 8, 4 and 2 millimeters and feeds of 0.25, 0.15, 0.10 and 0.05 mm/rev. During machining process, discontinuous, spiral, fragmented and continuous chips were obtained. Microstructural analysis determined that after cutting, they maintain a two-phase austenite-ferrite structure, where the grains become finer, from grain size number 5 for the standard sample, to number 10, for a number of revolutions of 125 rpm, an 8-millimeters cutting depth and feed of 0.25 mm/rev. It was grain size number 2 for 200 rpm; 4 mm depth and feed of 0.10 mm/rev which demonstrates that this decrease is due to the effect of work hardening. Microhardness analysis allow to established that when using a number of revolutions of 125 rpm, there is a hardness value of 387 HV and, for 200 rpm, the hardness is 365 HV, an increase attributed to the combined effect of friction, which generates work hardening.

Keywords: mechanical cutting, plastic deformation, cutting tool

Resumen: Se determinó el efecto del fenómeno del endurecimiento microestructural de las virutas deformadas con diferentes regímenes de corte en un acero AISI 4340 sometido al proceso de torneado. Se sometió a proceso de arranque de virutas una barra

del acero con números de revoluciones de 125, 150, 175 y 200 rpm; profundidad de corte de 8; 4 y 2 milímetros y avances de 0,25; 0,15; 0,10 y 0,05 mm/rev. Durante el proceso de mecanizado fueron obtenidas virutas del tipo discontinua, en espiral, fragmentadas y continuas, las cuales al realizar el análisis micro estructural se determinó que, luego del corte, mantienen una estructura bifásica de austenita-ferrita, donde los granos se hacen más finos, desde el número 5 para la muestra patrón, hasta el número 10, para número de revoluciones de 125 rpm, profundidad de corte de 8 milímetros y avance de 0,25 mm/rev, siendo del número de granos del número 2 para 200 rpm; 4 mm de profundidad y avance de 0,10 mm/rev, lo que demuestra que esta disminución es por el efecto de la acritud. Mediante el análisis de microdureza se estableció que, al emplear un número de revoluciones de 125 rpm, existe un valor de dureza de 387 HV y para 200 rpm, la dureza es de 365 HV, incremento al efecto combinado de la fricción, la cual genera la acritud.

Palabras clave: corte mecánico, deformación plástica, herramienta de corte

Introduction

Machining by chip removal is one of the most used processes in the industry. It is an important global manufacturing method with growing demand (Torres, 2020; Vergara, Ruiz-Huerta & Marín Calvo, 2021; Telenchana *et al*., 2024; Pulido de León *et al*., 2024). The aim of chip removal processes is achieving geometric shapes by removing excess material from the workpiece (Moreno, 2008; Tschätsch, 2009; Pulido-de León *et al*., 2024). Cutting tools wear the steel out forming varieties of metal chips, depending on the material and the type of wear used (Moya & Lara, 2019). According to Krahmer (2008) in chip removal processes, the degree of plastic deformation is high.

In the turning process, it is essential to consider a series of parameters existing in machining. The main objective is to cut the metal to obtain a specific shape and size, which is achieved by generating defined chips. The total absence of cutting fluid leads the mechanical energy introduced in the process to completely turn into heat (Durán, 2017). It is essential to find cutting parameters that ensure tool performance and the final dimensions of the machined part.

Steels are widely used due to their high temperatures and fatigue resistance properties; they contain additional elements, such as chromium and molybdenum, which improve

their hardenability, wear resistance, and toughness. 4340 steel includes chromium, nickel, and molybdenum, making it suitable for applications requiring high toughness (López-Castillo *et al*., 2024).

This work aims at determining the effect of microstructural hardening phenomenon on deformed chips with different cutting regimes in AISI 4340 steel subjected to a turning process.

Materials and Methods

Characterization of AISI 4340 steel

Table 1 shows the standard chemical composition of AISI 4340 steel, according to the designation adopted by AISI-SAE, of the American Society for Testing and Materials (ASTM).

Table 1. Chemical composition of AISI 4340 steel; % by mass

Steel	C	Mn	Cr	Ni	Mo	Si	S	P	Fe
AISI 4340	0,38-0,43	0.6-0.8	0.7-0.9	1.7-2.0	0.2-0.3	0.2-0.3	Max. 0.04	Max. 0.04	95.2-96.3

Machining is best performed with the steel in an annealed or normalized and tempered state. It can be easily machined by all conventional methods; however, under high strength conditions of 200 ksi or more, machinability is only 25% to 10% of that of the alloy in the annealed state (Gujimmy, 2023).

Orthogonal cutting model for chip formation

The chip is separated from the workpiece by a plastic deformation mechanism, corresponding to the relative displacement of the thickness elements. Furthermore, as the chip slides over the rake surface, a friction action between the chip and the tool is also manifested. The thermal interaction between the tool and the chip/workpiece set is part of the contact modelling (Grueso, 2009). In a cutting process, there are two main heat generation sources: by plastic deformation in the primary and secondary shearing zones and by friction in the tool-chip/workpiece contact zone. The model used for chip obtention, as shown in Figure 1, was the orthogonal cutting model (Durán, 2017).

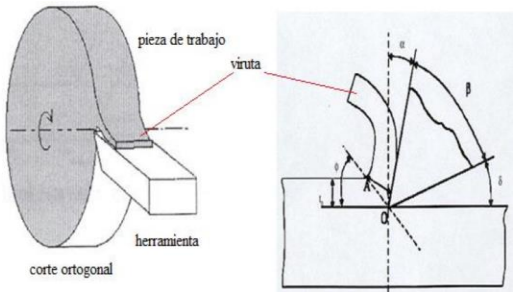

Figure 1. Orthogonal cutting model (Durán, 2017).

A universal lathe model 16K20 was used. The process was performed by machining an air-mounted workpiece, ensuring the length did not exceed twice the diameter of the workpiece. It was installed in a three-jaw self-centering chuck. A dry machining was performed.

Experimental planning for chip formation

Experimental planning is a structured process that allows determining the optimal conditions to obtain valuable information about a process or phenomenon, applying statistical methods to guarantee the validity and reproducibility of the results (Fernández, 1997). Table 2 shows the experiments´ planning matrix.

Table 2. Experiments planning matrix

	Variable			**Output**			**Output**		
	n_r (rpm)	T (mm)	S (mm/r)	H(HV)			Microestructura		
-	12	12	0,10						
Δ	18	10	0,28						
+	120	4	0,20						
Tests	Experimental Runs								
1	**-**	**-**	**-**	HV1	HV2	HV3	M1	M2	M3
2	**Δ**	**Δ**	**Δ**	HV1	HV2	HV3	M1	M2	M3
3	**+**	**+**	**+**	HV1	HV2	HV3	M1	M2	M3

To determine steel´s final microhardness and microstructure, machining experiments were carried out using different process variables combinations. Each combination of variables was tested three times (replicates), resulting in a total of 12 experimental runs.

Characterization of the equipment used in the experiments

Within the design processes, cutting of samples must be performed meticulously. For microstructural tests, non-alteration of the material properties is vital, as their alteration reflect a distorted image.

In the optical microscope, different filters are used to improve contrast and emphasize specific characteristics based on the material's properties. This is achieved with magnifications typically ranging from 2.5 to 1,000. In materialography, reflected light is the most common type used in optical light microscopes. Transmitted light optical microscopes are also used, although primarily for mineralogy samples (Struers, 2024).

An EchoLAB IM500 optical microscope was used, equipped with a camera installed via the IMI.VIDEOCAPTURE.exe hardware, which displays the image on the computer. The microstructure of the standard specimen was observed, which will be used for comparison with the micrographs obtained after the machining process with different feed rates, cutting depths, and rotational speeds.

Samples encapsulation in thermosetting phenolic resin

Due to the need to perform roughing and polishing operations, the samples were encapsulated to facilitate their handling (Figure 2).

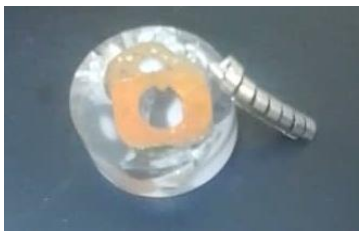

Figure 2. Chip encapsulation.

Metallographic samples polishing

For roughing, a flat and semi-polished surface must be obtained using machine tools and abrasive papers. The sample was rotated when moving from one abrasive to another to completely erase the marks from the previous one.

After concluding this process, the fine polishing operation is carried out, using "Pasta GOI" abrasive paste, applied on discs provided with mops. This polishing was performed manually on a felt surface to avoid rounding the sample edges.

Angles that could break the emery paper were removed. The sanding stages were performed with sandpaper. For fine sanding process, it was used 600, 800, and 1,200 grain-sized sandpapers, as shown in Figure 3, completely removing the marks from the previous sandpaper. When changing from one sandpaper to another, new scratches, perpendicular to the previous ones, were obtained. Chromium oxide was used for the final polish. Once polished, the test pieces were washed with distilled water and dried with filter paper.

Figure 3. Metallographic samples fine sanding.

Metallographic preparation

The procedures to prepare the chips samples obtained from the machining process of AISI 4340 steel were carried out:

1) Material selection
2) Sample cutting
3) Specimen mounting
4) Chemical etching of the test piece
5) Microscopic analysis
6) Micrograph obtention

Calculation of cutting regimes for turning

The cutting regimes' fundamental parameters are tool feed, number of revolutions, cutting speed, and cutting depth (López, Ruiz & Colás, 2001).

Calculation of cutting speed

The speed at which the workpiece rotates in the lathe is an important factor and can influence production volume and cutting tool lifespan. A very low lathe speed will cause loss of time; a very high speed will cause the tool to lose its edge.

$$Vc = \frac{\pi \cdot D \cdot n}{1\,000}$$

Where:
Vc: cutting speed; m/min
D: workpiece diameter; mm
n: number of revolutions; rpm
1000: conversion factor from meters to millimeters

Facing operation

This consists of cleaning the front faces of the workpiece. The basic or machining time for this operation is calculated by the following equation:

$$Tm = \frac{\frac{D}{2}+Y+\Delta}{n \cdot s} i$$

$Y = t \cos \cdot \varphi$

D: 1…3

Where:
Y: blade entry length; mm
φ: Coefficient
i: number of passes

Test pieces machining time of the

The machining time for the test pieces is the time invested by the operator to perform the work, also known as basic time or total machining time.

$$Tm = \frac{L}{n \cdot s} \cdot i$$

Where:
Tm: machining time; min.
L: length to machine; mm.
S: feed; mm/rev

For a successful machining process, the tool must offer a consistent and predictable performance, ensuring that the desired results are reliably achieved. The tool must be wear-resistant, minimizing interruptions in the machining process.

Taylor's equation allows predicting the tool lifespan on the base of the cutting speed (Vc) (Erazo-Arteaga, 2024). This relationship is exponential, meaning that a small change in cutting speed can have a significant impact on tool lifespan.

$$V_c T^{nf} = C$$

Where:
T: tool lifespan, min
nf: exponent that depends on the cutting conditions, in this case between 0,2 and 0,5.
C: cutting speed corresponding to a 1-minute lifespan.

The influence exerted by the selected variables on the cutting tool and the different machining conditions on their lifespan is determined from the cutting regimes. The parameters for determining the tool span are established in table 3.

Table 3. Parameters to determine tool lifespan

No.	n (rpm)	t (mm)	S (mm/r)	T (min)	nf	Vc (m/min)	C
1	12	8	0,10	12	0,35	Vc1	C1
2	18	8	0,28	10	0,35	Vc2	C2
3	120	5	0,20	4	0,35	Vc3	C3

Feed is the parameter with the greatest influence *nf* on the tool lifespan for the machined workpiece. Its increase indicates the tool has better characteristics regarding wear resistance.

The combination of cutting conditions, tool material, and workpiece material, influence quantifiably the Taylor´s equation constants. The types of chips produced significantly affect the surface finish and the general cutting conditions.

Results and Discussion

Analysis of the machining regimes

To determine the effect of hardening through the microstructural behavior of the different chips obtained, the orthogonal cutting parameters were calculated. Table 4 shows the cutting parameters that allowed obtaining the different types of chips.

Table 4. Cutting parameter results

	Variables			**Results**				
	n_r (rpm)	**t(mm)**	**s (mm/r)**	**Vc (m/s)**	**Tm_{ref} (min)**	**i**	**Y**	**Tmt (min)**
1	125	8	0,25	14,1	2,24	3	8	14,2
2	150	8	0,15	16,9	1,86	3	8	12
3	175	4	0,10	19,7	1,60	3	4	10,2
4	200	2	0,05	22,6	1,40	3	2	9

With high cutting speeds (14.1 m/min), a thickness reduction in the primary deformation zone was observed. Chemical elements, such as sulfur, can promote formation of manganese sulfide inclusions, which act as stress concentrators in the matrix. However, their effect as stress concentrators is limited to low and medium cutting speeds.

How ease the material is removed represents economy in the component production. Chemical elements also influence the machining process; sulfur, mainly, promotes the formation of manganese sulfide inclusions, which act as stress raisers in the chip shear plane, embrittling it and initiating crack formation, in addition to decreasing the chip-tool contact length. The stress concentration generated by the inclusions depends on factors such as: quantity, size, hardness, shape, and distribution.

According to Kudo (1965) and Dewhurst (1978), who have also conducted studies to establish relationships between the cutting force (among other cutting parameters) and

the morphology, size, shape, and distribution of inclusions; the inclusions effect as stress concentrators in the matrix is limited to low and medium cutting speeds, decreasing their effect as speed increases.

Microhardness analysis

Since chip removal is performed by the penetration of a tool, whose material has greater hardness (60 HRC) than the workpiece to be cut (170 HB), during friction and pressure, the effect of work hardening influences the material's hardness. Table 5 shows the microhardness results.

Table 5. Obtained microhardness results

	Variables			H(HV)		
	Nr (rpm)	t(mm)	s(mm/r)		Output	
1	125	8	0,25	387	387	388
2	150	8	0,15	367	367	368
3	175	4	0,10	377	377	378
4	200	2	0,05	365	365	366

For a 125-rpm speed, there is higher hardness than for 200 rpm; the increase in hardness is presumably associated with the cutting depth parameter, the first is 8 millimeters and the last 2 millimeters. With greater depth and a slower machine movement, greater deformation is achieved in the material. Moreover, two other parameters are included: dry machining and temperature, the latter increasing with longer friction time. Under the first condition, thicker chips are also obtained.

Microstructural analysis for 125 rpm, t = 8mm and S = 0,25 mm/rev

Figure 4 corresponds to the microstructural analysis for 125 rpm, 8 mm depth and feed of 0.25 mm/rev. Two observations were made to avoid influences from an anomalous measurement.

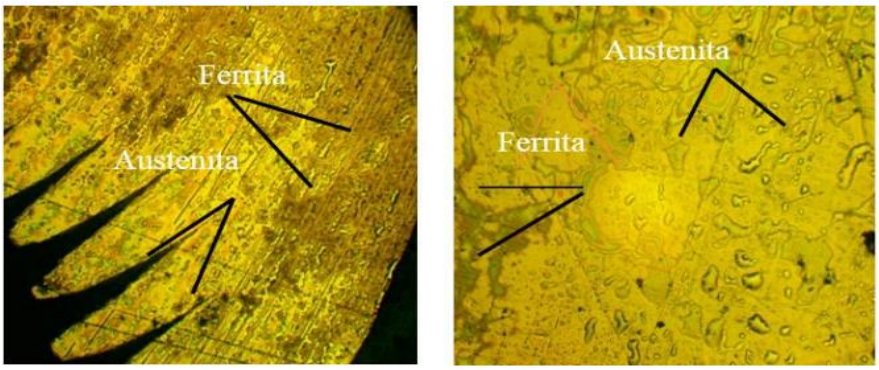

Figure 4. a) 1st observation. b) 2nd observation.

According to Vargas (2022), microstructures show different grain crystalline orientations, which contribute to the activation of a set of slip systems and become an active system that determines the grain's deformation and local stresses levels and, consequently, the deformation at the macroscopic level. In the observed samples, from Figure 5 (a) to Figure 5 (b), a microstructure formed by Austenite and Ferrite is observed.

Microstructural analysis for 150 rpm, t = 7 mm and S = 0.15 mm/rev

In the case of contact with high pressures, the friction value, measured for a pair of materials that are in contact, depends on several parameters, mainly the level of applied pressure but also the temperature at the interface and the relative sliding velocity of one solid with respect to the other. These parameters influence the chip's segmented morphology since segmentation phenomenon heightens when the fraction of heat transmitted to the chip intensifies. Likewise, when heat dissipation in the chip increases, the chip's radius of curvature is smaller, this phenomenon is related to a more prominent fragmentation of the chip (Lamorú-Urgelles *et al.*, 2024).

Figure 5 shows the microstructural behavior resulting from the machining at 150 rpm, with 8 mm depth of cut and a 0,15 mm/rev feed rate. Figure 5 shows the microstructure resulting from machining at 150. At this level, a lower clustering of grains (number 7) can be appreciated. In these microstructures, the effect of textures is less relevant in the proximities of the area corresponding to the deformation.

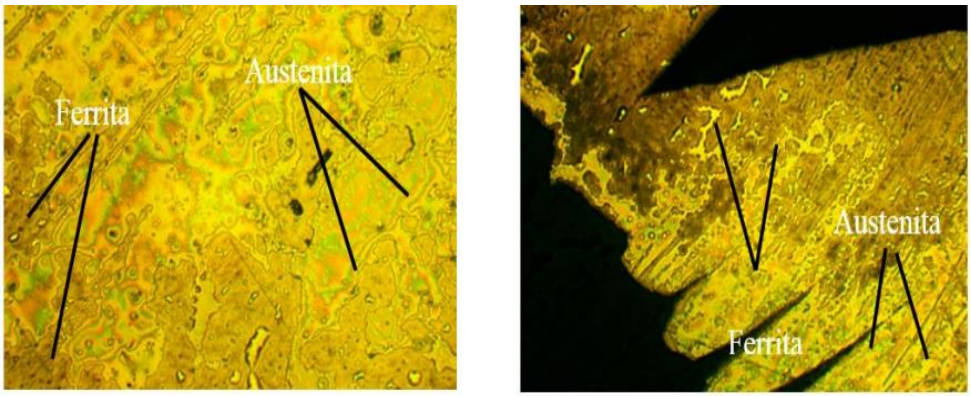

Figure 5. a) 1st observation. b) 2nd observation.

Microstructural analysis for 175 rpm, t = 4 mm and S = 0.10 mm/rev

The number of revolutions was increased to 175 rpm and the feed was decreased, as these two parameters are inversely proportional. Figure 6 shows the microstructural behavior obtained from the machining process with parameters of 175 rpm, 4 millimeters depth and feed of 0,10 mm/r.

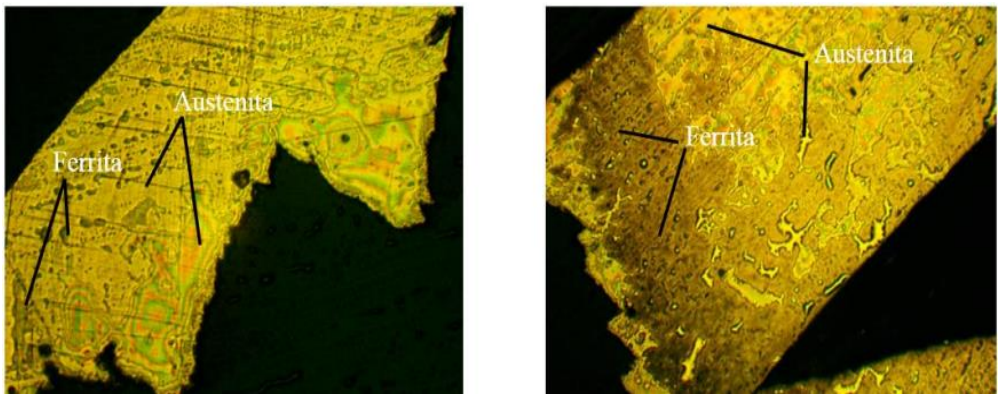

Figure 6. a) 1st observation. b) 2nd observation.

The microstructures correspond to the fragmented chip type. Under these machining conditions, the chips break, leaving the workpiece surface with a poor finish. In these cases where the feed was considerable and the cutting depths were low, the chip shape is discontinuous. When increasing the number of revolutions, the cutting depth is significant and causes a vibration effect in the machine and changes the cutting-edge temperature. If this temperature changes rapidly, cracks may appear in a perpendicular direction to the cutting edge, associated with intermittent cuts.

Microstructural analysis for 200 rpm, t = 2 mm and S = 0.05 mm/rev

Microstructural variations were obtained for machining at 200 rpm, a depth of 2 millimeters, and a feed of 0.05 mm/rev (Figure 7).

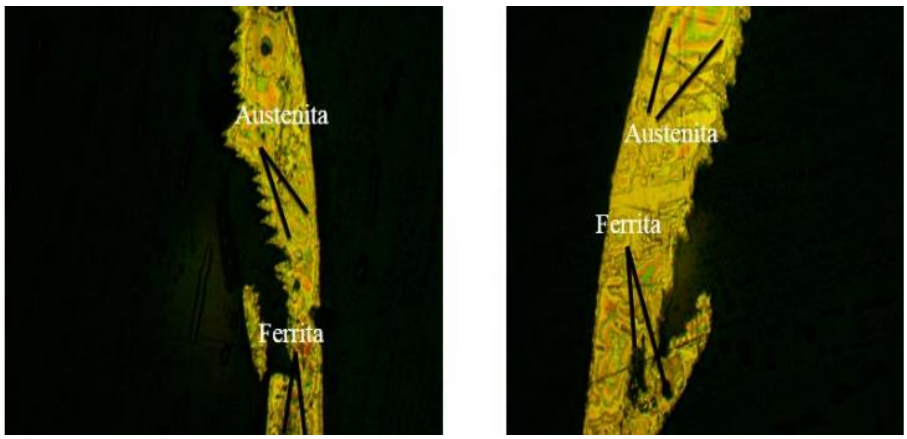

Figure 7. a) 1st observation. b) 2nd observation.

For the number of revolutions´ maximum magnitude, greater grain deformation is observed in the direction of chip sliding over the tool. The samples maintain the same two-phase composition, but denser with better grain rearrangement. It can be assumed that the plastic deformation is accommodated by slip.

The activation of the different systems is strongly associated with the critical activation stresses, and the plastic anisotropy depends on the relationship between the introduced deformation levels. Intracrystalline slip occurs with lower stresses since crystals are not perfect, they have defects that help achieving an increase in deformation.

During the machining process, discontinuous, spiral, fragmented, and continuous chips were obtained. With a microstructural analysis it was determined that after cutting, they maintain a two-phase austenite-ferrite structure.

Conclusions

It is established that variations in different machining parameters significantly influence chip formation and the wear of the tool's cutting edge when in contact with the workpiece interface, thereby requiring longer machining time for the workpiece.

Through the microstructures obtained by varying the rotation speed, cutting depth, and feed, the effect of work hardening on AISI 4340 steel subjected to different dry cutting conditions is determined.

It was established that cutting considers friction as a phenomenon of material shearing within the chip along the contact zone, and they form in correspondence with the generation of temperature and friction.

Bibliographic References

Dewhurst, P. (1978). On the non-uniqueness of the machining process. *Proceedings of the Royal Society of London. A. Mathematical and Physical Sciences*, 360(1703), 587-610. https://royalsocietypublishing.org/doi/abs/10.1098/rspa.1978.0087

Durán, A. (2017). *Determinación del fenómeno de la acritud en virutas deformadas durante el proceso de torneado*. (Degree Thesis, University of Moa, Cuba). http://ninive.ismm.edu.cu/handle/123456789/2310

Fernández, L. (1997). *Metodología de la planificación experimental.* (Doctoral Dissertation, Universidad Ramon Llull, España). https://dialnet.unirioja.es/servlet/tesis?codigo=11928

Erazo-Arteaga, V.A., Mejía-Echeverría, C. & Umaquinga, A.C. (2024). Metodologías para la predicción de la vida útil en herramientas de corte por arranque de viruta. Una revisión bibliográfica*. Estudios y perspectivas. Revista Científica y Académica,* 4(3), 1972-2989. https://estudiosyperspectivas.org/index.php/EstudiosyPerspectivas/article/view/524

Grueso, J. M. (2009). Estudio del desempeño de herramientas de corte de acero rápido convencional y acero rápido sinterizado en la industria metalmecánica. *Revista Clepsidra,* *5*(9), 51-72. http://revistas.fuac.edu.co/index.php/clepsidra/article/download/206/192

Gujimmy. (2023). *What is 4340 Steel*. Acero Waldun. https://waldunsteel.com/es/que-es-acero-4340/

Krahmer, D. M. (2008). Procesos de arranque de viruta y no convencionales que se aplican en la industria metalmecánica. *Argentina: Instituto Nacional de Tecnología Industrial, Mecánica*.

Kudo, H. (1965). Some new slip-line solutions for two-dimensional steady-state machining, *International Journal of Mechanical Science,* 7(1), 43-55. https://doi.org/10.101670020-7403(65)90084-6

Lamorú-Urgelles, M., Fernández-Columbié, T., Cañete-Utria, M., Leyva-Tarafa, M. & Pérez-Lamorú, M.L. (2024). Modificaciones en las estructuras de un acero al carbono y un acero estructural por efecto del ciclo térmico. *Ciencia & Futuro, 14*(3), 361-374. https://revista.ismm.edu.cu/index.php/revistacyf/article/download/2596/1982

López-Castillo, J. M., Arroyo-Vázquez, Á. E., Arriola-Landaverde, M. O., Montemira-Mávil L.A., González-Lira, Y. G., Alarcón-Castañeda, A. & Gamboa-López, S. G. (2024). Parámetros para mejorar y asegurar la calidad en los tratamientos térmicos. *BASACHÍ 2*(2), 47-54.

López, F.E., Ruiz, M. & Colás, R. (2001). Modelaje de la viruta en el proceso de maquinado. *Ingenierías,* IV(13), 40-47. http://eprints.uanl.mx/10062/1/13_Eugenio_Lopez_Modelaje_de_la_V.pdf

Moreno, L.M. (2008). *Materiales industriales. Teoría y aplicaciones*. ITM

Moya, J. C., & Cando Lara, L. F. (2019). Análisis de las prioridades físicas y mecánicas del hormigón elaborado con fibras de acero reciclado. *INGENIO*, *1*(2), 5–14. https://doi.org/10.29166/ingenio.v1i2.1623

Pulido-de León, L. A., García-Treviño, I. L. Medina-Álvarez, M. A. & De Los Santos-Méndez, F. (2024). Optimización del plan de mantenimiento preventivo para equipos de mecanizado por arranque de viruta mediante análisis de fiabilidad y costos. *Ciencia Latina, 8*(5), 4759-4780. https://doi.org/10.37811/cl_rcm.v8i5.13929

Struers (2024). *Microscopio metalográfico*. https://www.struers.com/es-ES/Knowledge/Microscopy#microscopyhowto

Telenchana, L.S., Hernández, C.M., Robayo, M.D. & Muñoz. G.R. (2024). Impacto ambiental de los procesos industriales de mecanizado por arranque de viruta con tornos paralelos mediante métodos innovadores: revisión del estado del arte. *Concienciadigital,* *7*(2), 126-140. https://concienciadigital.org/revistacienciadigital2/index.php/ConcienciaDigital/article/view/2993

Torres, J. S. (2020). Obtención de nanoparticulas de óxido de hierro procedente de viruta con tecnología BOTTOM–UP. *Revista De Ciencia, Tecnología E Innovación*, *18*(21). https://doi.org/10.56469/rcti.v18i21.365

Vargas, L. (2022). *Análisis microestructural del acero AISI/SAE A2 tratado térmicamente.* (Master´s Thesis, University of Antioquia, Colombia). https://bibliotecadigital.udea.edu.co/handle/10495/25984

Vergara, D. Ruiz-Huerta, L. y Marín Calvo, N. (2021). Definición de metodología para la fabricación de material compuesto a base de polietileno de tereftalato y virutas metálicas, *Apanac*, 156-162. https://revistas.utp.ac.pa/index.php/apanac/article/view/3068